FAST NUMERICAL CALCULATIONS OF 3-D PHASED ARRAY WAVE FIELDS BASED ON TRANSIENT POINT SOURCE SYNTHESIS

Frank SCHUBERT, Bożena LAMEK
FRAUNHOFER IZFP, Dresden, Germany.

1. INTRODUCTION

The increasing interest in ultrasonic phased array techniques for non-destructive evaluation (NDE) and structural health monitoring (SHM) applications is based on the fact that reasonably priced and easy-to-use transducers and multi-channel measuring systems become more and more available. As a consequence the need for fast and reliable modelling tools for the design and optimization of phased array wave fields is also increasing. While semi-analytical methods for wave field synthesis are usually very fast but often suffer from several approximations like neglect of near-field effects, multiple scattering, and mode conversions, purely numerical methods include all relevant wave phenomena but are characterized by significantly larger computation times and memory requirements, especially in 3-D. In the present paper a new hybrid method is presented which combines the Elastodynamic Finite Integration Technique (EFIT) with the concept of transient point source synthesis. As a result broadband 3-D ultrasonic wave fields generated by arrays of connected and distributed transducers can be calculated within a few seconds on a common PC. We present various examples of application including high-frequency phased arrays for volume inspection and low-frequency guided wave arrays. We also discuss how the proposed technique can be expanded to multi-layers and anisotropic media.

2. TRANSDUCER WAVE FIELD MODELING

The modeling of ultrasonic wave fields can be performed by two different kinds of techniques, namely (semi-)analytical and purely numerical methods, respectively. While numerical methods like the elastodynamic finite integration technique (EFIT, [1,2]) or the mathematically similar finite difference time domain (FDTD) technique [3] are discretizing the volume of the model region and are typically working in the time domain, (semi-)analytical methods based on point-source-synthesis (PSS), Green's functions, and integral transformations, respectively, are usually discretizing outer and inner boundaries of the model and are mostly working in the frequency domain [4,5].
Numerical techniques are based on the wave equation and thus, include the whole wave physics. They are particularly used for complex set-ups where an accurate treatment of all existing wave modes including multiple scattering, mode conversions, surface and interface waves etc. is necessary. Their main disadvantage however, is the large amount of memory and computation time requirements, especially in high-frequency 3-D applications. (Semi-)analytical methods on the other hand are significantly faster but usually neglect certain aspects of the wave field like surface and interface waves, multiple scattering etc. and are thus restricted to relatively simple model geometries. Transducer modeling in general can be seen as a high-frequency 3-D problem and was therefore dominated by (semi-)analytical techniques in the past. In the present paper the elastodynamic finite integration technique is combined with point-source-synthesis in order to expand the area of application of the EFIT method and to allow a fast and accurate time-domain simulation of transient 3-D transducer wave fields.

3. TRANSIENT WAVE FIELD OF A POINT SOURCE

The starting point of the proposed technique is the wave field of a normal force point source acting on a linearly elastic isotropic medium with stress-free or motion-free boundary conditions. Analytical solutions are available for the elastic half space as well as for the elastic plate problem. Further approaches for multilayered structures can also be found in the literature but evaluation of the corresponding equations is complex in general and has to be done numerically. Moreover, most of

these techniques are usually working in the frequency domain and provide time harmonic monochromatic solutions.
In order to calculate more realistic time-domain solutions, the axisymmetric version of the elastodynamic finite integration technique based on cylindrical coordinates is a valuable tool. This so called CEFIT technique can be used for arbitrarily layered systems by using one and the same fully numerical framework [6]. Due to the curvilinear coordinate system, axisymmetric 3-D problems like normal force point sources can be effectively reduced to 2-D models in the r/z-plane with moderate memory and computation time requirements. In Fig. 1, a time snapshot of the elastic wave field caused by a broadband point source (frequencies up to 3 MHz) acting on a steel half space with stress-free boundary conditions is shown. The data for the v_r and v_z velocity components form the basis for the subsequent point-source-synthesis (PSS). It should be noted that the wave field can be calculated for different points in time and thus, the full spatio-temporal data can be used for PSS purposes after it has been calculated and saved to a storage medium.

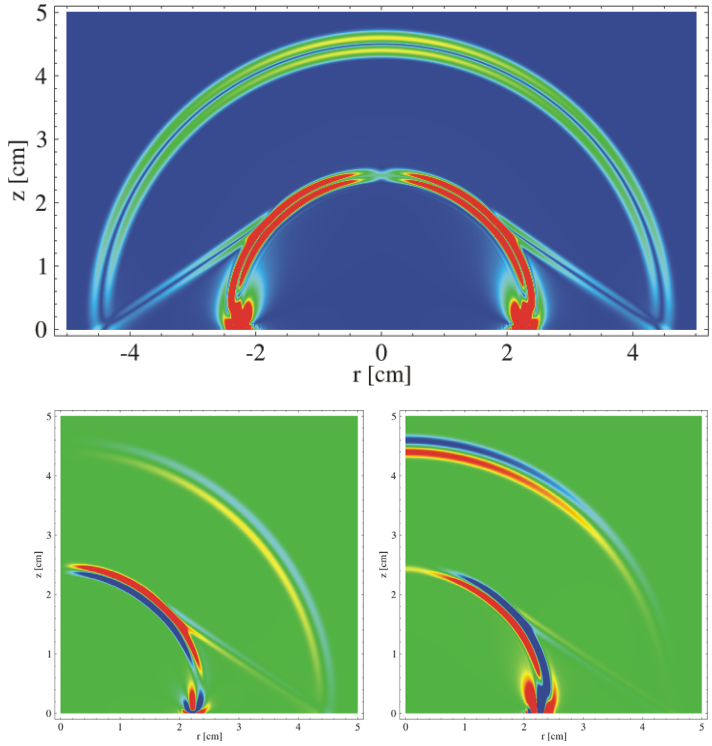

Figure 1: *Result of axisymmetric EFIT simulation of a wave field generated by a broadband point source acting on a steel half space. Top: absolute value of particle velocity; bottom: v_r (left) and v_z velocity component (right).*

4. TRANSIENT POINT SOURCE SYNTHESIS

After performing the axisymmetric CEFIT calculation, the model region around a circular aperture with a diameter of 2 cm was discretized by using a Cartesian xyz coordinate system. Its origin coincides with the center of the circular aperture while the latter stretches across the x-y plane. For each space point the velocity components v_x, v_y, and v_z have been calculated by summing up the contributions of all point sources lying inside the transducer aperture. For each pair of space and source point the corresponding radial and axial coordinates, *r* and *z*, have been determined and used to extract the existing CEFIT data.
The results of this EFIT-PSS combination are shown in Fig. 2 and are compared to a pure CEFIT calculation in which the finite aperture has been explicitly taken into account. The agreement between the two calculations is very good although the spatial discretization of the EFIT-PSS model is four times smaller than that of the pure CEFIT model. Moreover, the 3-D EFIT-PSS calculation time is nearly two orders of magnitude smaller than the time for the quasi 2-D CEFIT calculation.

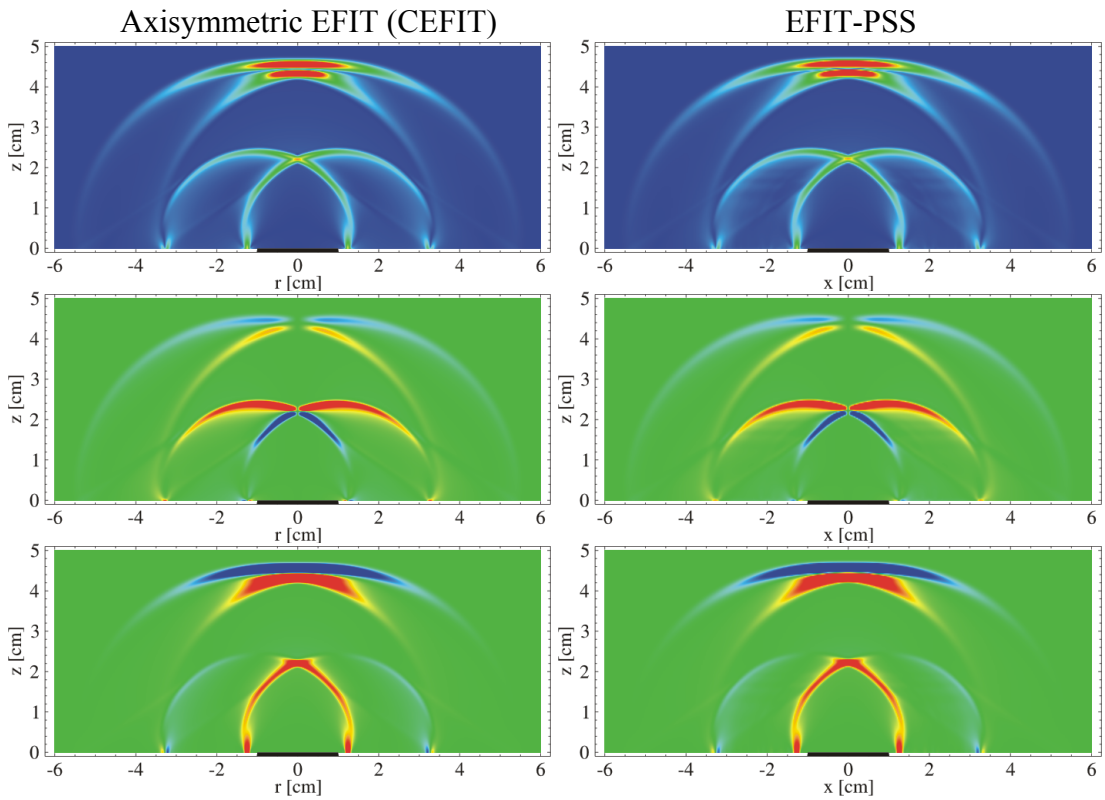

Figure 2: *Comparison of results for the circular piston transducer (r-z/x-z cross-sections through the origin at y = 0). Left column: axisymmetric EFIT calculation; right column: EFIT-Point-Source-Synthesis. The agreement is very good although the spatial discretization of the EFIT-PSS model is four times smaller than for the axisymmetric EFIT model.*

Beside the cross-sections through the origin at y = 0 as shown in Fig. 2 one can also calculate arbitrary cross-sections in the x-z and x-y plane according to the full three-dimensional nature of the EFIT-PSS solution [7].

The preceding problem of a circular piston can be directly calculated with the quasi 2-D CEFIT code and was only presented to demonstrate the general principle of the new method and to validate it against the corresponding CEFIT solution. A rectangular transducer element, however, is out of reach for the pure EFIT technique since it requires the calculation of full 3-D wave fields leading to very large memory requirements and unacceptably long calculation times. By using the hybrid EFIT-PSS method the solution can be obtained within a few seconds on a common PC.
Fig. 3 shows the results for x-z and y-z cross-sections through the origin showing the wave field of a rectangular transducer element with a width of 1.5 mm in x- and 8 mm in y-direction. Such an element is often used in linear phased-array probes. As can be seen from the pictures there is nearly no focusing of the P wave in the x-z plane since the corresponding width of the transducer element is smaller than the dominating wavelengths. In the y-z plane, however, a significant focusing can be observed that comes along with two shear and Rayleigh wave fronts generated by the edges of the radiating element.
Fig. 4 additionally shows the EFIT-PSS results in an x-y cross-section at z = 42 mm. The size of the transducer element is indicated by the black rectangle. The higher amplitudes in x-direction caused by the larger aperture in y-direction are clearly visible.

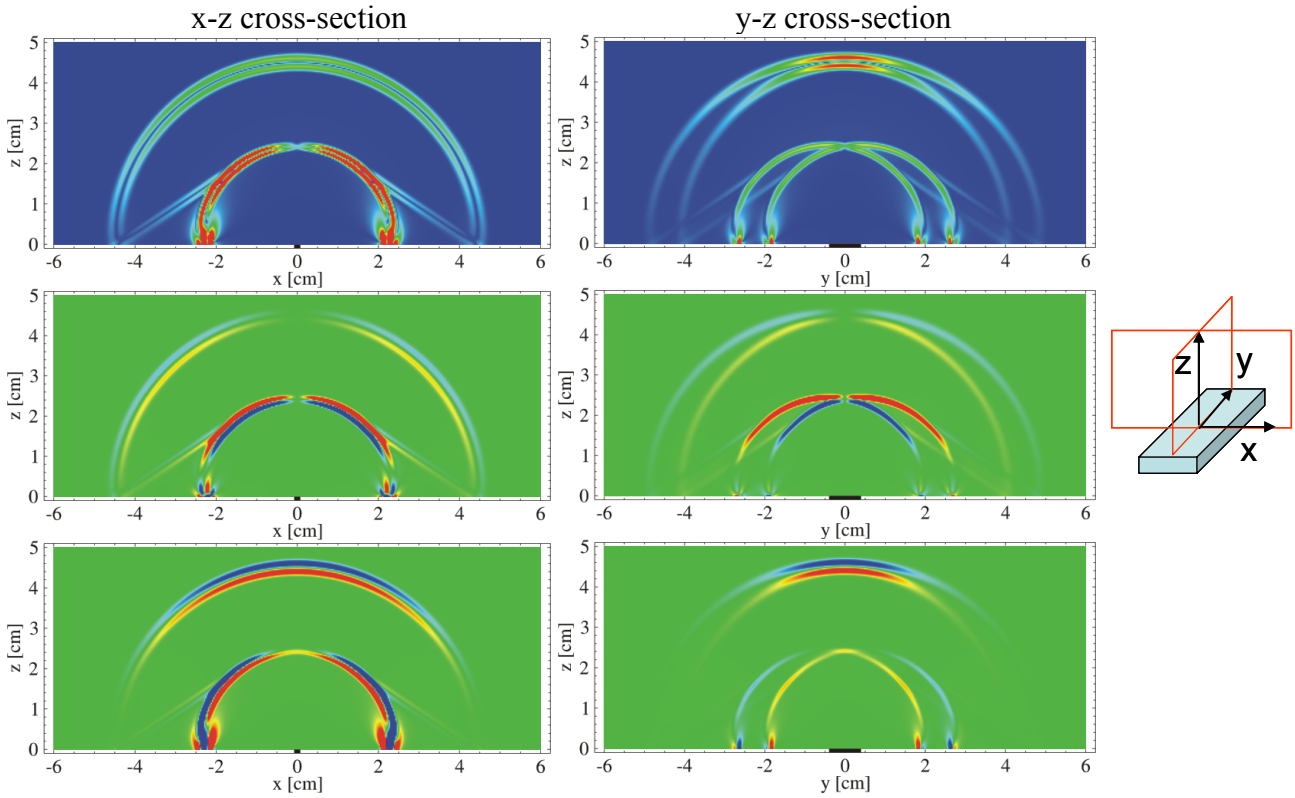

Figure 3: *EFIT-PSS results for the rectangular piston transducer (x-z cross-sections (left column) and y-z cross-sections through the origin (right column)). First row: absolute value of particle velocity; second row: v_x component; third row: v_z component. The transducer width amounts to 1.5 mm in x- and 8 mm in y-direction.*

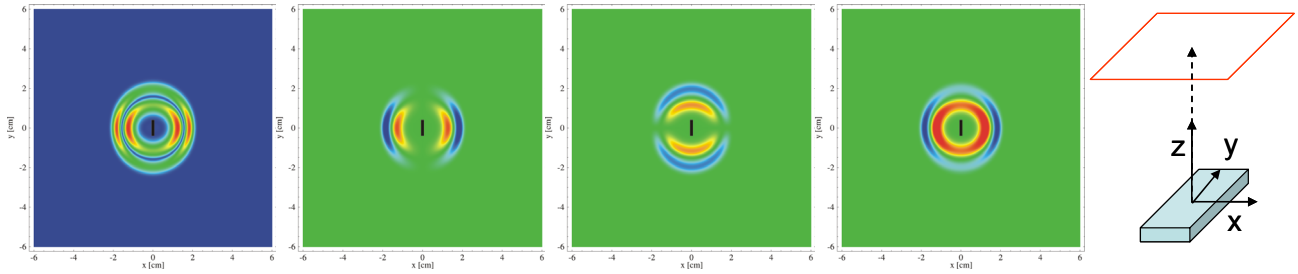

Figure 4: *EFIT-PSS results for the rectangular piston transducer (x-y cross-sections at z = 42 mm). From left to right: absolute value of particle velocity, v_x component, v_y component, v_z component. The size of the transducer element is indicated by the black rectangle.*

5. PHASED ARRAY WAVE FIELDS

In chapter 4 only a spatial point source synthesis (PSS) for single element transducers was described but the initial point source calculation (Fig. 1) provides the full spatio-temporal wave field and thus, also more complex angle-beam and phased array transducers can be modelled by using the EFIT-PSS approach. Fig. 5 shows cross-sectional snapshots of the wave field of a focused 17 MHz linear phased array, having a focal depth of 2.5 mm and a beam angle of 30°. In Fig. 6 the wave field of the same transducer but with a beam angle of 0° with respect to the vertical is shown.

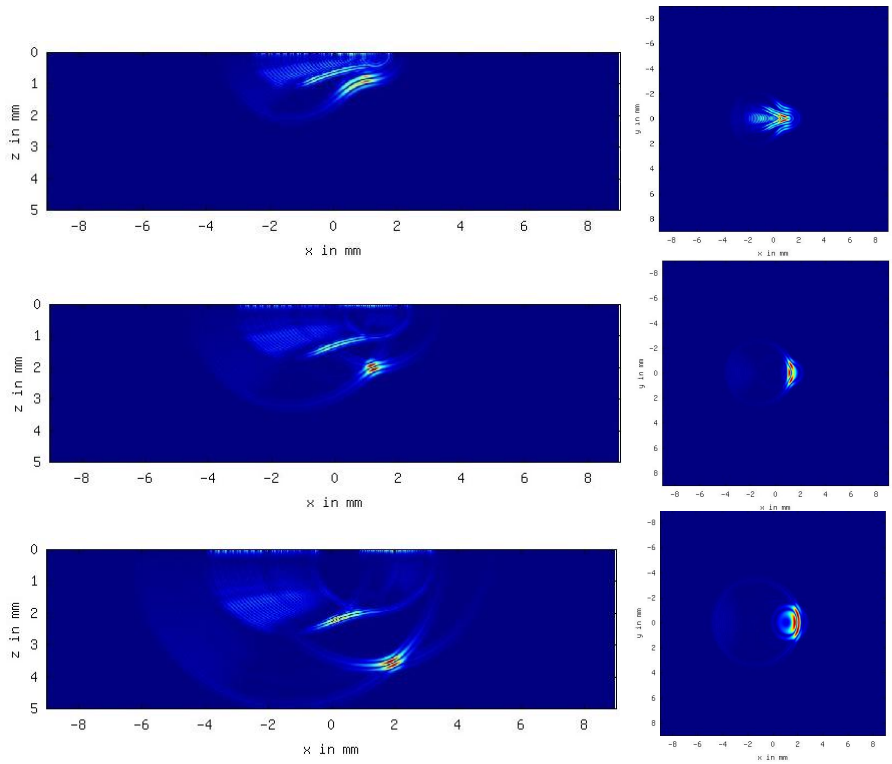

Figure 5: *Wave front snapshots of a 17 MHz linear phased array with a focal depth of 2.5 mm and a beam angle of 30° as calculated by the EFIT-PSS technique. On the left: x-z cross section at y =0; on the right: x-y cross section through the current position of the main wave front. From top to bottom: t = 0.25 µs, t = 0.42 µs, t = 0.67 µs. In each case the absolute value of the particle velocity is displayed.*

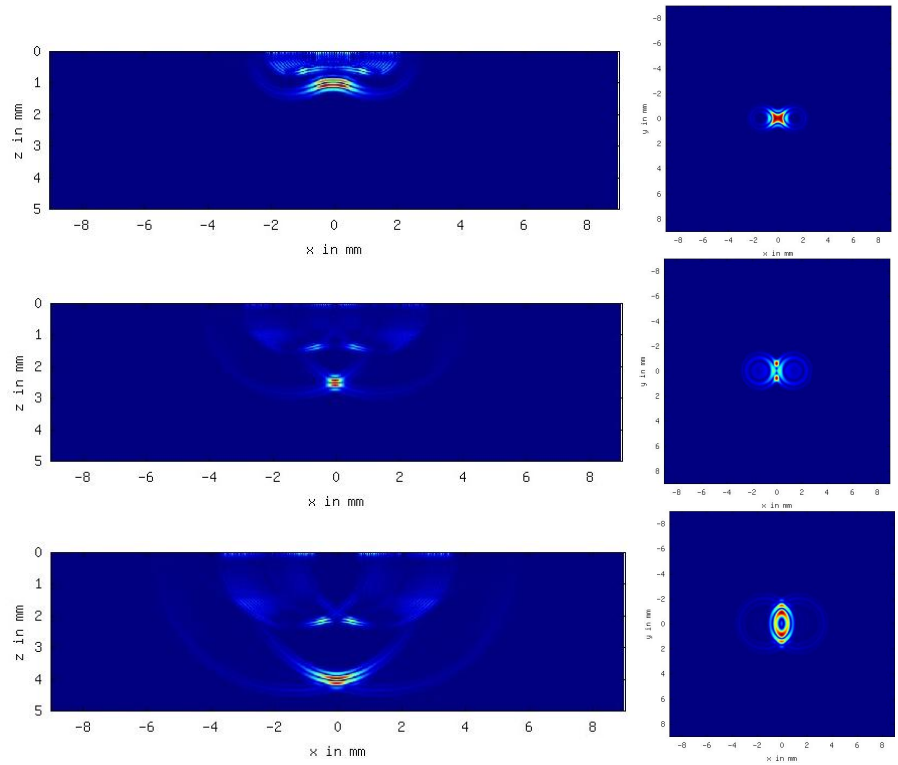

Figure 6: *Wave front snapshots of a 17 MHz linear phased array with a focal depth of 2.5 mm and a beam angle of 0° as calculated by the EFIT-PSS technique. On the left: x-z cross section at y = 0; on the right: x-y cross section through the current position of the main wave front. From top to bottom: t = 0.17 µs, t = 0.42 µs, t = 0.67 µs. In each case the absolute value of the particle velocity is displayed.*

6. LAMB WAVE SYNTHESIS

One important option for structural health monitoring (SHM) and non-destructive evaluation (NDE) of plate- and shell-like structures is based on the application of guided ultrasonic waves generated and detected by arrays of connected or distributed transducers. Similar to the half-space problem in the preceding chapters we can start with the transient wave field of a point source generating guided waves due to the presence of a second free parallel surface. Since for guided waves the wavelengths are typically not smaller than the plate thickness it is usually sufficient to store the spatio-temporal wave field along one surface of the plate only because this 2-D wave field is already representative for the 3-D wave field across the full plate thickness. Only in cases where both lower and higher frequencies and thus, Lamb waves and Rayleigh waves are simultaneously present, a full 3-D PSS reconstruction makes sense. Therefore, in the following examples we restrict ourselves to a quasi 2-D PSS along the upper plate surface but keep in mind that the 3-D character of the initial wave field is included.

In Fig. 7 the B-Scan data of the elastic wave field due to a normal point source (center frequency = 200 kHz) acting on a 4 mm thick aluminum plate with stress-free boundary conditions is shown. The fast symmetric Lamb wave S0 and the slower antisymmetric A0 mode can clearly be identified. The spatio-temporal data for the v_r and v_z velocity components along the top surface of the plate form the basis for the subsequent point-source-synthesis.

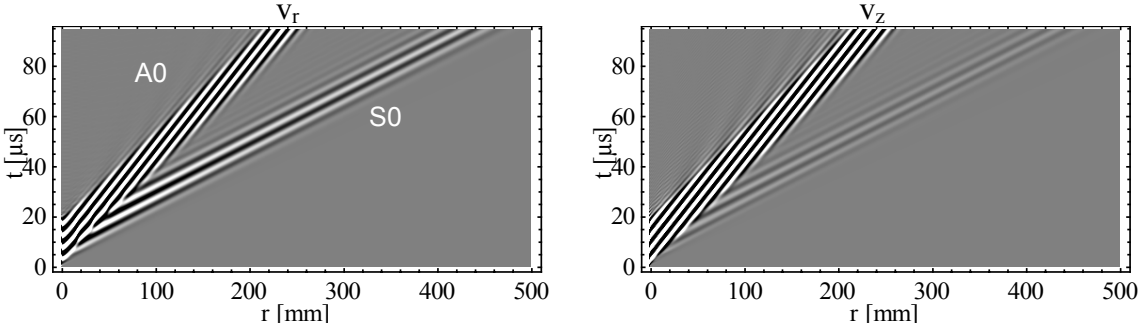

Figure 7: *B-Scan data of an axisymmetric EFIT simulation of a Lamb wave field generated by a normal point source acting on a 4 mm thick aluminum plate (c_P = 6260 m/s, c_S = 3080 m/s, ρ = 2700 kg/m³). On the left: radial component of particle velocity (v_r); on the right: axial component of particle velocity (v_z).*

In Fig. 8 the corresponding time domain signals obtained at r = 170 mm are shown. One can see that the normal point source generates a strong A0 but only a weak S0 wave.

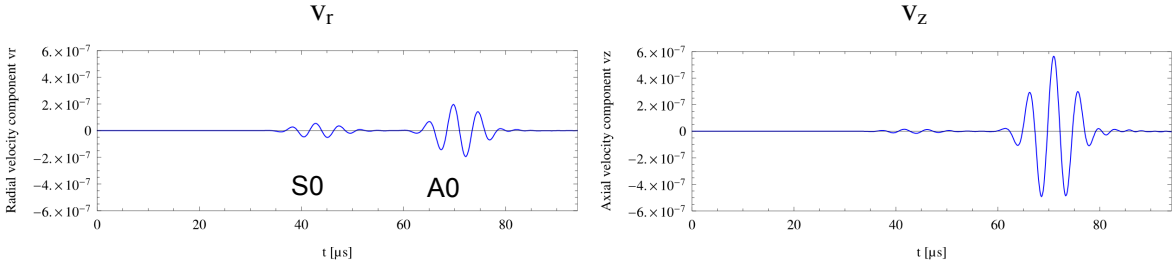

Figure 8: *A-Scan data at r = 170 mm of axisymmetric EFIT simulation of a Lamb wave field generated by a normal point source acting on a 4 mm thick aluminum plate. On the left: radial component of particle velocity (v_r); on the right: axial component of particle velocity (v_z).*

After performing the axisymmetric CEFIT calculation of the elementary point source, the resulting wave field due to a finite transducer aperture can simply be calculated by summing up the contributions of various point sources lying inside the aperture. The result of this EFIT-PSS combination for a circular aperture with a radius of 5 mm is shown in Fig. 9. The absolute value of the particle velocity vector shows that the S0 wave is significantly stronger compared to the point source in Fig. 8. However the A0 wave is still dominant due to the normal force excitation used here.

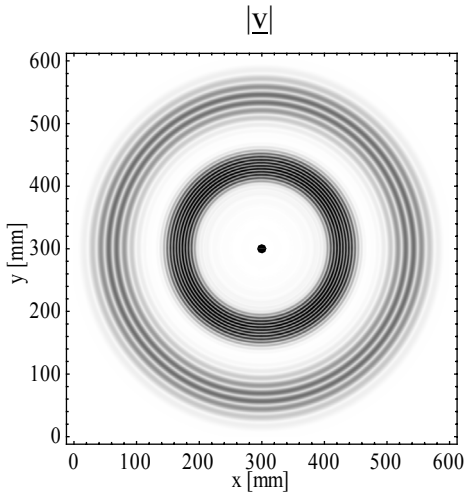

Figure 9: *EFIT-PSS result for a circular transducer element with a radius of 5 mm. The picture displays the absolute value of the particle velocity vector, $|\underline{v}|$.*

In Fig. 10 (left-hand side) a rectangular (square) transducer element with a lateral size of 15 mm has been used for the transient point-source synthesis. As a result the A0 wave is predominantly excited in the x and y directions while a characteristic gap appears in 45° directions. In contrast to the A0 wave the S0 mode is not significantly affected due to its larger wavelength. Its corresponding wave field is obviously isotropic.
In order to test the accuracy of the EFIT-PSS procedure the wave field of the rectangular aperture was compared with the results of a 3-D EFIT calculation of the same problem. Since the 3-D EFIT code has been successfully validated in the past [8] it can serve as a reference for the new method.

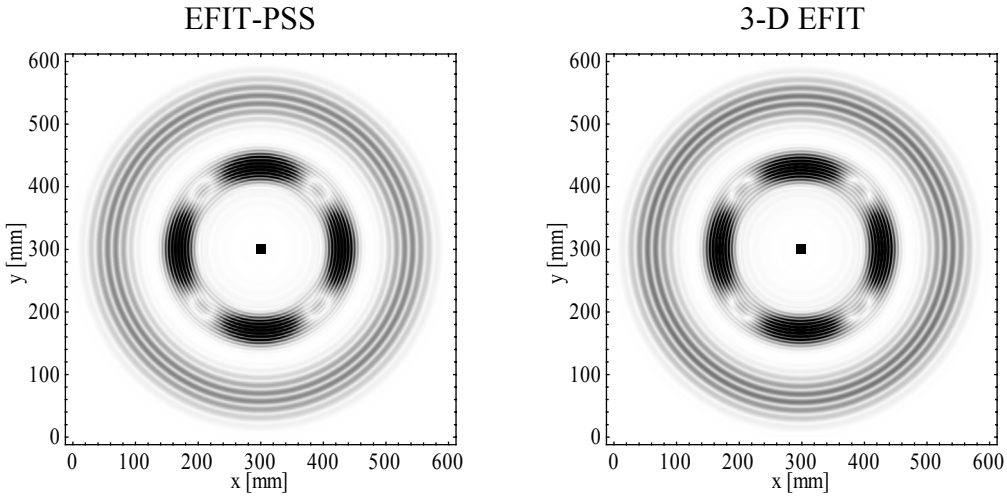

Figure 10: *Comparison of EFIT-PSS (left-hand side) and 3-D EFIT result (right-hand side) for a square transducer element with a lateral size of 15 mm showing a very good agreement. However, the EFIT-PSS calculation needs 600 times less computer memory and is 100 times faster than the corresponding 3-D EFIT calculation.*

The right picture of Fig. 10 shows the result of the 3-D EFIT calculation. The agreement between the two calculations is very good. Slight differences in the A0 wave front are caused by its extremely short wavelengths and can be avoided by a finer discretization of the 3-D EFIT and/or the EFIT-PSS reconstruction grid. However, it is important to point out that the EFIT-PSS calculation needed approximately 600 times less computer memory and was approximately 100 times faster than the corresponding 3-D EFIT calculation.

Fig. 11 shows another example in which the wave field of a rectangular transducer element with a size of 30 mm in x- and 15 mm in y-direction is shown. In this case the v_y velocity component is displayed and the agreement between 3-D EFIT and EFIT-PSS calculation is excellent demonstrating the accuracy of the transient point source synthesis.

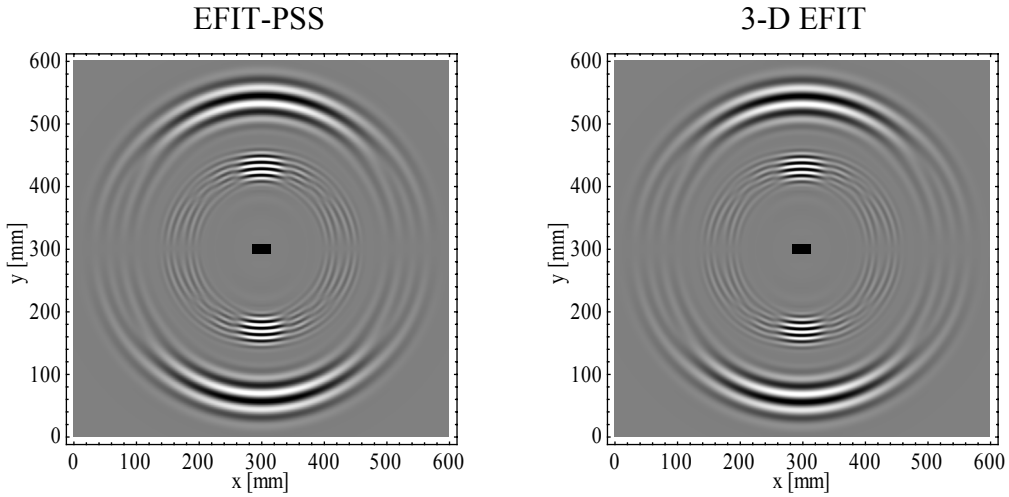

Figure 11: *Comparison of EFIT-PSS (left-hand side) and 3-D EFIT results (right-hand side) for a rectangular transducer element with a size of 30 mm in x- and 15 mm in y-direction. Both pictures display the v_y velocity component. The agreement between the two calculations is excellent.*

7. LAMB WAVE ARRAYS

If a number of transducer elements is combined to a multi-channel array the resulting Lamb wave fields can be simply varied by changing the temporal excitation of the single elements. In the following example we calculated the Lamb wave field of a linear array of 16 circular transducer elements with a radius of 3.3 mm and a distance of 6.6 mm to each other. In order to produce both, a strong S0 and a strong A0 wave, radially vibrating transducers were used in this case. In order to further speed up the point-source-synthesis the wave field of a complete circular transducer element instead of a single point source has been calculated by the CEFIT technique and used as the reference wave field for the synthesis. The corresponding B-Scan data and a typical A-Scan calculated at r = 170 mm is shown in Figs. 12+13.

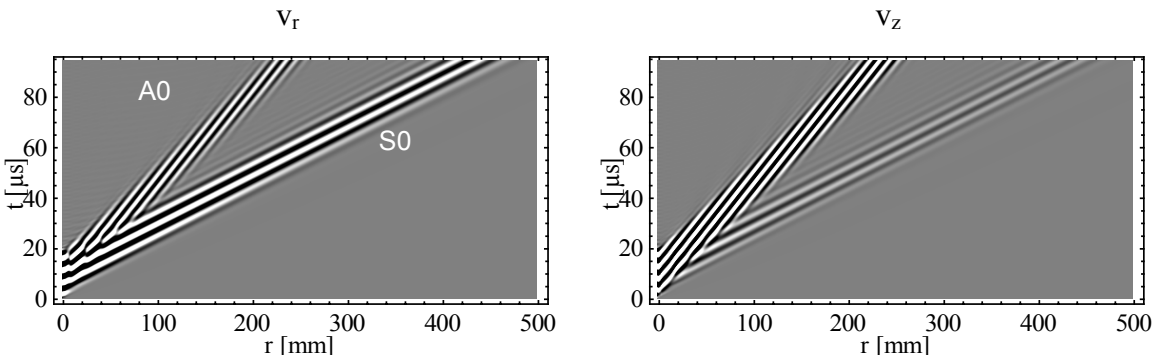

Figure 12: *B-Scan data of axisymmetric EFIT simulation of a Lamb wave field generated by a radially vibrating circular transducer with a radius of 3.3 mm. On the left: radial component of particle velocity (v_r); on the right: axial component of particle velocity (v_z).*

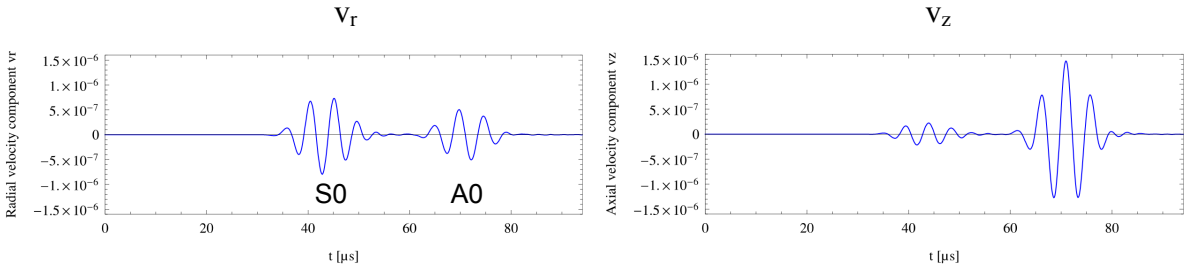

Figure 13: *A-Scan data at r = 170 mm of an axisymmetric EFIT simulation of a Lamb wave field generated by a radially vibrating circular transducer with a radius of 3.3 mm. On the left: radial component of particle velocity (v_r); on the right: axial component of particle velocity (v_z).*

By using specific time delays between the 16 single transducer elements the wave fields of S0 and A0 modes can be steered and focused to nearly arbitrary directions or focal points. In Fig. 14 a constant time delay of $\Delta t = 1.24$ µs has been used. In this case the strongest S0 wave is propagating to the left while the A0 wave is steered in a direction of approx. 60° with respect to the array axis. More examples can be found in [9].

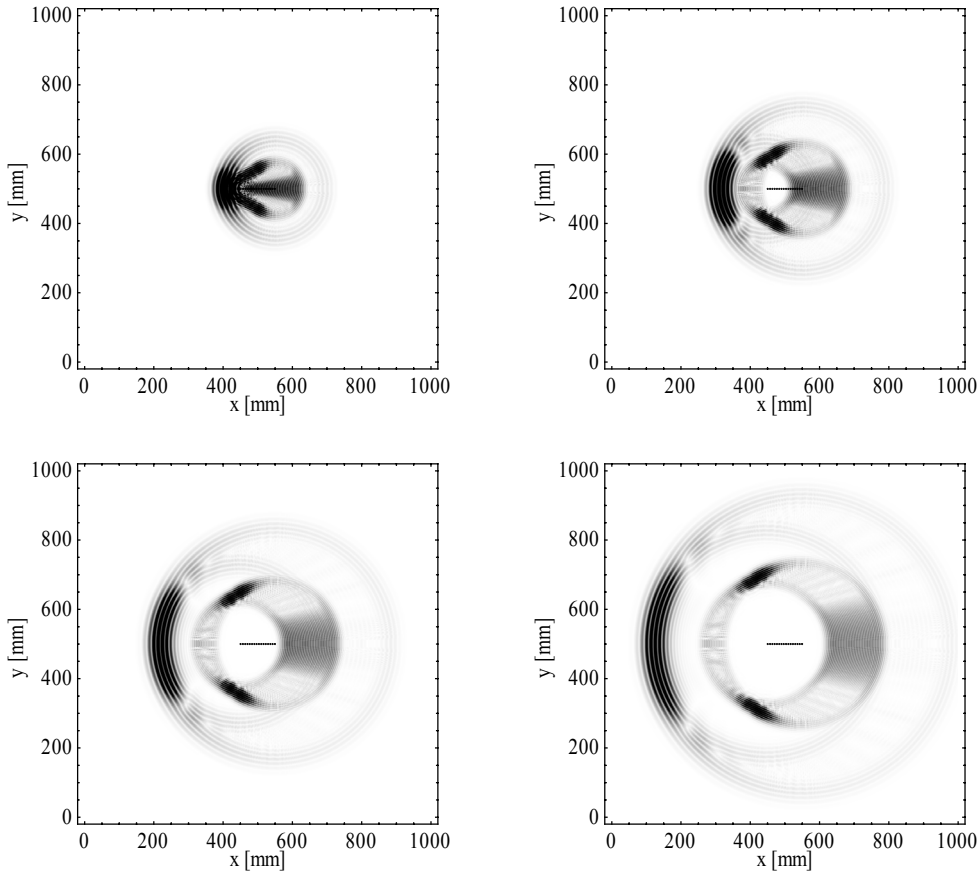

Figure 14: *EFIT-PSS snapshots for a linear array of 16 radially vibrating circular transducers with a radius of 3.3 mm and a distance of 6.6 mm to each other. A constant time delay of $\Delta t = 1.24$ µs is used between the single elements.*

8. FURTHER EXTENSIONS

By using the EFIT-PSS technique wave fields of nearly arbitrary transducer configurations like linear, matrix, circular and distributed arrays can be calculated. For normal force excitation and radially vibrating circular transducers the axisymmetric CEFIT can be used to obtain the initial wave field. For other kinds of sources like shear-horizontal excitation and for anisotropic media the initial CEFIT calculation must be replaced by a single 3-D EFIT calculation with appropriate boundary and symmetry conditions. This data can then be used to calculate the wave field of various trans-

ducer geometries without the need for further numerical 3-D calculations.
The initial 3-D calculation is also necessary if guided wave propagation in cylindrical shells is investigated. In this case no axisymmetric source is available. However, the wave field of different transducer configurations can be reconstructed by transient point-source- synthesis using a similar procedure as explained in this paper for plates. For both plates and shells the formalism can also be extended to multi-layered systems as exemplary described in [7] for body waves.

9. CONCLUSIONS

In the present paper the hybrid EFIT-PSS technique that combines the advantages of the numerical EFIT technique and a transient point-source-synthesis has been presented. With this time-domain approach, 3-D wave fields for various transducer and array configurations can be easily calculated with only a fraction of the computational effort needed for full numerical 3-D calculations. The typical gain in computer memory requirements lies between 500 and 1000%, while the computational speed-up factor amounts to 100 at least.
In particular the following relevant transducers can be calculated with the new EFIT-PSS method: Circular piston transducers, annular transducers, annular phased arrays, rectangular transducers, linear phased arrays, square transducers, matrix phased arrays, piezo composite transducers, angle beam probes and laser ultrasonic apertures.
The EFIT-PSS results can be presented as wave front snapshots for different points in time, wave front animations, time-domain signals at arbitrary positions (A-, B-, C-Scan representations) and the well-known intensity plots. The proposed technique is not restricted to axisymmetric isotropic problems since the basic point source data can also be calculated by using a single 3-D calculation of an arbitrarily layered isotropic or anisotropic material. This initial data can then be used to calculate the wave field of various transducer geometries without the need for further numerical 3-D calculations. As a conclusion one can summarize that the proposed EFIT-PSS technique represents a significant extension of the EFIT framework establishing a powerful time-domain tool for the design and optimization of a variety of transducer set-ups. In particular it can be expected that the proposed technique will lead to a significant improvement of phased array wave fields since the complete broadband time-domain data from each single transducer element can be taken into account in order to optimize the spatio-temporal wave field synthesis.

REFERENCES

[1] F. Schubert, “Numerical time-domain modeling of linear and nonlinear ultrasonic wave propagation using finite integration techniques – Theory and applications”, Ultrasonics **42**, 221-229, 2004.
[2] P. Fellinger, R. Marklein, K.-J. Langenberg, S. Klaholz, “Numerical modeling of elastic wave propagation and scattering with EFIT- elastodynamic finite integration technique”, Wave Motion **21**, 47-66, 1995.
[3] Y.-H. Chen, W. C. Chew, and Q.-H. Liu, “A three-dimensional finite difference code for the modeling of sonic logging tools”, J. Acoust. Soc. Am. **103** (2), 702-712, 1998.
[4] M. Spies, “Transducer-Modeling in General Transversely Isotropic Media Via Point-Source-Synthesis: Theory”, J. of Nondestr. Eval. **13** (2), 85-99, 1994.
[5] E. Kuehnicke, “Optimization of Ultrasound Broadband Transducers for Complex Testing Problems by Means of Transient and Time Harmonic Sound Fields”, In. Proc. of 9th European Conference on NDT, Berlin 2006, BB 103-CD, Poster 154, DGZfP 2006.
[6] F. Schubert, A. Peiffer, B. Köhler, T. Sanderson, “The elastodynamic finite integration technique for waves in cylindrical geometries“, J. Acoust. Soc. Am. **104** (5), 2604-2614, 1998.
[7] F. Schubert, B. Lamek, “3-D Ultrasonic Transducer Modeling Using the Elastodynamic Finite Integration Technique in Combination with Point-Source-Synthesis”, In: Proceedings of 4th International Workshop ‘NDT in Progress’, November 7-9, 2007, Prague, Czech Republic, A1-A10, 2007.
[8] F. Schubert, B. Koehler, “Three-dimensional time domain modeling of ultrasonic wave propagation in concrete in explicit consideration of aggregates and porosity“, Journal of Computational Acoustics, Vol. **9**, No. 4, 1543-1560, 2001.
[9] F. Schubert, B. Lamek, “Efficient Calculation of Guided Wave Phased Array Wave Fields Based on Symmetry Principles”, Proc. 5th Workshop “NDT in Progress”, October 12-14, 2009, Prague, Czech Republic, 271-280, 2009.